us to control the position of the Fermi level ε_F and change the values of its electrokinetic characteristics.

In [3], the authors showed that the structure of the base semiconductor *TiCoSb* is defective. Thus, there are vacancies (Va) (~ 1%) in the crystallographic position 4*a* of *Ti* atoms, and additional *Co** atoms (up to ~1%) are located in the tetrahedral voids of the structure, which occupy ~24% of the unit cell volume [2]. As result, the formula of the *TiCoSb* semiconductor is transformed into $(Ti_{0.99}Va_{0.01})Co(Co^*_{0.01})Sb$. Vacancies generate structural defects of acceptor nature in position 4*a* of *Ti* atoms, and the corresponding acceptor band ε_A appears in the band gap ε_g. Additional *Co** atoms generate defects of donor nature in the tetrahedral voids of the semiconductor structure, and the donor band ε_D appears in the band gap ε_g.

All described above explains the nature of the mechanism of simultaneous "a priori" doping of the initial *TiCoSb* semiconductor by donor and acceptor impurities, which makes it heavily doped and highly compensated [4]. Taking into account that the Fermi level ε_F in *TiCoSb* lies within the band gap between the states of ionized donors and acceptors, the changes in the ratio between them caused, for example, by the modes of thermal annealing of samples and their cooling, purity of initial components, etc., will shift the position of the Fermi level ε_F relative to impurity bands and continuous energies bands. For this reason, the compound *TiCoSb* is a semiconductor of the hole-type conductivity at temperatures $T < 90$ K, which is indicated by positive values of the Seebeck coefficient α, and at higher temperatures the majority carriers are electrons. This temperature dependence of the type of the majority carriers also indicates a different depth of energy levels: the acceptor states are smaller and ionized at lower temperatures than the donor ones.

Semiconductor thermoelectric materials based on *TiCoSb* were reported in [3-9]. Thus, in $Ti_{1-x}V_xCoSb$ and $Ti_{1-x}Mo_xCoSb$ semiconductors, structural defects of acceptor nature are simultaneously generated as vacancies in the positions of *Ti* and *Co* atoms, and occupation of 4*a* positions of *Ti* atoms by *V* or *Mo* atoms generates defects of donor nature. The mechanism of simultaneous appearance of acceptors and donors provides the semiconductor properties of $Ti_{1-x}V_xCoSb$ and $Ti_{1-x}Mo_xCoSb$. Doping of *TiCoSb* by *Sc* atoms ($3d^14s^2$) introduced by substitution of *Ti* atoms ($3d^24s^2$) generates structural defects of acceptor nature in $Ti_{1-x}Sc_xCoSb$ (*Sc* atom has fewer 3*d*-electrons than *Ti*), and the ratio of defects of donor and acceptor nature determines the position of the Fermi level ε_F in the band gap ε_g and the mechanisms of electrical conductivity.

The study of the semiconductor thermoelectric material $TiCo_{1-x}Ni_xSb$ revealed a linear variation in the value of the unit cell parameter a(*x*), which indicates the substitution of *Co* atoms by *Ni* ones. In this case, donors are generated in the crystal, because the *Co* atom ($3d^74s^2$) has a smaller number of 3*d*-electrons than the *Ni* atom ($3d^84s^2$). The thermoelectric material $TiCo_{1-x}Cu_xSb$ has a different behaviour of structural parameters depending on the impurity concentration.

The presented results of studying the electrokinetic and energy characteristics of the semiconductor solid solution $TiCo_{1-x}Mn_xSb$, $x = 0.01$–0.10, as well as their comparison with the results of modeling the electronic structure, will help to identify the mechanisms of electrical conductivity in order to determine the conditions of synthesis of thermoelectric materials with maximum efficiency of thermal energy into electrical energy conversion.

Investigation procedures

$TiCo_{1-x}Mn_xSb$ samples were synthesized by arc-melting the charge of the constituent components (the content of the main component not less than 99.9 wt.%) in an electric arc furnace in

an inert atmosphere followed by homogenizing annealing for 720 h at 1073 K. Excess 1–3 wt. % *Sb* was used to compensate for losses during the electric arc-melting procedure. The chemical and phase compositions of the samples were examined by X-ray phase (DRON-4.0 diffractometer, *Fe*K*α* radiation) and metallographic analyses (TESKAN VEGA 3 LMU electron microscope equipped with an X-ray analyzer with energy dispersion spectroscopy (EDRS)). The structural parameters of the solid solution $TiCo_{1-x}Mn_xSb$ samples were calculated using the Fullprof Suite program [10]. Modeling of the electronic structure of $TiCo_{1-x}Mn_xSb$ was performed by the KKR method (Corringa-Kohn-Rostoker method) in the approximation of the coherent potential CPA and local density LDA [11]. Licensed software AkaiKKR and SPR-KKR in the LDA approximation for the exchange-correlation potential with Moruzzi-Janak-Williams (MJW) parameterization were used for KKR calculations [12]. The Brillouin zone was divided into 1000 *k*-points, which were used to model energy characteristics by calculating DOS. The width of the energy window was 22 eV and was chosen to capture all semi-core states of p-elements. The full potential FP in the representation of plane waves was used in the calculations by the linear MT orbital method. The LDA approximation with MJW parameterization was used as the exchange-correlation potential. The accuracy of calculating the position of the Fermi level is ± 4 meV. Temperature and concentration dependences of electric resistivity (ρ) and the Seebeck coefficient (α) relative to copper of $TiCo_{1-x}Mn_xSb$ were measured in the ranges: T = 80–400 K, x = 0.01–0.10.

Research on structural characteristics of $TiCo_{1-x}Mn_xSb$

Microprobe analysis of the concentration of atoms on the surface of $TiCo_{1-x}Mn_xSb$ samples established their correspondence to the initial compositions of the charge (Fig. 1), and X-ray phase and structural analyses showed that the powder patterns of samples, including the composition x=0–0.10, are indexed in the *MgAgAs* structure type and contain no traces of other phases. (Fig. 2a).

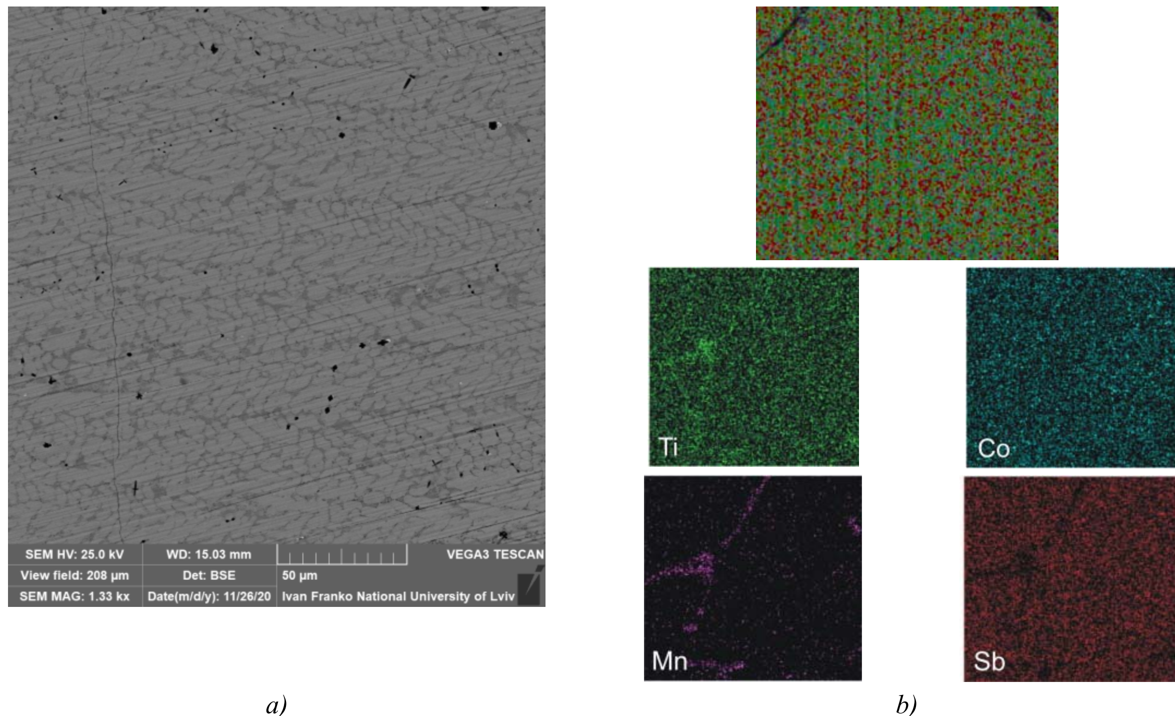

a) b)

Fig. 1. Photograph of the surface (a) and distribution of elements (b) in the sample $TiCo_{0.95}Mn_{0.05}Sb$

Structural studies of $TiCo_{1-x}Mn_xSb$ solid solution revealed the complex character of the inclusion of impurity *Mn* atoms into the semiconductor structure matrix. Since the atomic radius of *Mn* (r_{Mn} = 0.130 nm) is larger than that of *Co* atom (r_{Co} = 0.125 nm), then the increase of the unit cell parameter a(x) of $TiCo_{1-x}Mn_xSb$ in the concentration range x = 0–0.05 is logical (Fig. 2b). Such behavior of the parameter a(x) should indicate the realization of $TiCo_{1-x}Mn_xSb$ substitutional solid solution, where structural defects of acceptor nature are generated in the crystallographic site 4*c* of *Co* atoms. In this case, an impurity acceptor band ε_A^{Mn} should be formed in the band gap ε_g of the semiconductor.

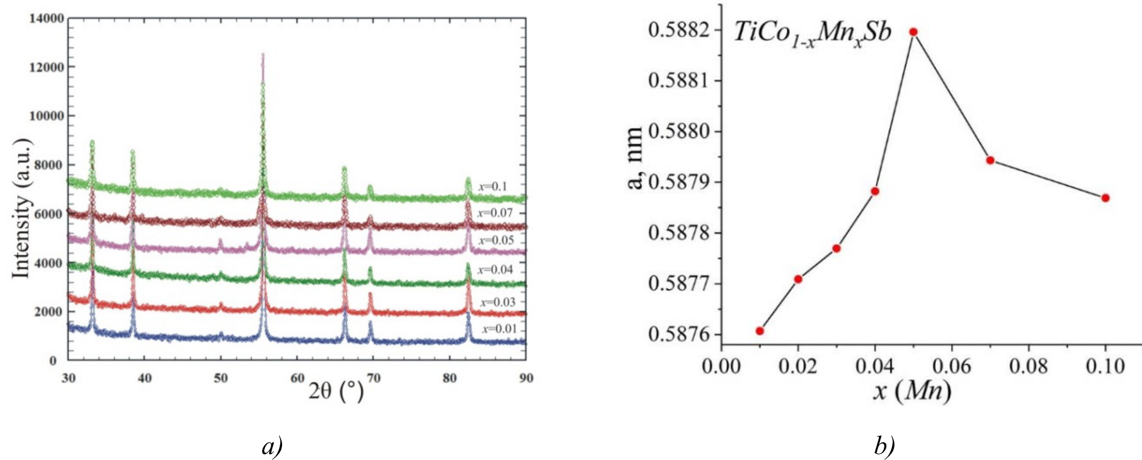

a) *b)*

*Fig. 2. X-ray powder diffraction patterns of samples (**a**) and variation of the unit cell parameter a(x) (**b**) for* $TiCo_{1-x}Mn_xSb$

However, the appearance of an extremum on the dependence a(x) of $TiCo_{1-x}Mn_xSb$ at $x = 0.05$, followed by a decrease of the unit cell parameter a(x) at $x > 0.05$ do not fit into the logic of forming a substitutional solid solution when *Co* atoms are replaced by *Mn* atoms. Thus, if the concentration of impurity *Mn* atoms at $x = 0.05$ would be the limit of the existence of solid substitution (the limit of solubility of these atoms in the semiconductor structure matrix), then the value of the unit cell parameter a(x) of $TiCo_{1-x}Mn_xSb$ should not change significantly. At the same time, the decrease in the values of a(x) of $TiCo_{1-x}Mn_xSb$ at $x > 0.05$ indicates the existence of a substitutional solid solution, but now the impurity *Mn* atoms occupy a different crystallographic position. In this connection, it is worth reminding the study of $Ti_{1-x}V_xCoSb$ semiconductor [8], where the authors found the fact of simultaneous occupation of *V* ($3d^34s^2$) impurity atoms both in the 4*a* crystallographic position of *Ti* atoms, which generated structural defects of donor nature (*V* atom contains more electrons than *Ti* atom) and in the 4*c* position of *Co* atoms, which generated defects of acceptor nature (*V* has fewer 3*d*-electrons than *Co*).

The most probable in $TiCo_{1-x}Mn_xSb$ at $x > 0.05$ is the occupation by the *Mn* atoms of the crystallographic position 4*a* of the *Ti* atoms. Indeed, since the atomic radius of the *Mn* atom is smaller than that of *Ti* (r_{Ti} = 0.146 nm), the decrease of the unit cell parameter a(x) for $TiCo_{1-x}Mn_xSb$ at $x > 0.05$ (Fig. 2b) becomes clear. In this case, structural defects of donor nature will be generated in crystallographic position 4*a* (*Mn* atoms have a larger number of 3*d*-electrons than *Ti*), and the impurity donor band ε_D^{Mn} should be formed in the band gap ε_g of the $TiCo_{1-x}Mn_xSb$ semiconductor.

We can assume that in a real $TiCo_{1-x}Mn_xSb$ crystal these processes occur simultaneously, but the rate of substitution of certain atoms depends on the concentration of impurity *Mn* atoms. At lower concentrations of *Mn* atoms ($x \leq 0.05$) they replace *Co* atoms to a greater extent, and at $x > 0.05$ – *Ti*

atoms. Herewith, donors and acceptors are generated simultaneously at different rates in $TiCo_{1-x}Mn_xSb$, and the semiconductor becomes heavily doped and highly compensated (HDHCS) [13].

However, taking into account the small number of impurity *Mn* atoms dissolved in the structure matrix of the initial semiconductor, as well as the poor accuracy of the X-ray method of studying the structure, we failed to record any other structural changes.

Thus, structural studies of the semiconductor thermoelectric material $TiCo_{1-x}Mn_xSb$ showed a complex mechanism of impurity inclusion into the semiconductor matrix. The results of experimental investigations of electrokinetic properties for $TiCo_{1-x}Mn_xSb$ will show the correspondence of the conclusions to the real processes in the crystal.

Investigation of the electronic structure of $TiCo_{1-x}Mn_xSb$

To predict the behavior of the Fermi level ε_F, the band gap ε_g, and the electrokinetic characteristics of the $TiCo_{1-x}Mn_xSb$ semiconductor, the distribution of density of electronic states (DOS) was calculated (Fig. 3) for an ordered variant of the structure when *Ti* atoms are substituted by *Mn* atoms in the crystallographic position 4*a*. From Fig. 3 we can see that in the base *TiCoSb* semiconductor the Fermi level ε_F lies near the middle of the band gap ε_g, but closer to the edge of the conduction band ε_C. Since the substitution of *Co* atoms by *Mn* ones generates structural defects of acceptor nature, already at the concentration of $TiCo_{0.99}Mn_{0.01}Sb$ the Fermi level ε_F will drift from the conduction band ε_C and will be located in the middle of the band gap ε_g. At higher concentrations of the acceptor impurity, the concentration of acceptors will increase, and the Fermi level ε_F will approach, and then will cross the percolation level of the valence band ε_V of $TiCo_{1-x}Mn_xSb$, and the dielectric-metal conduction transition will occur [14].

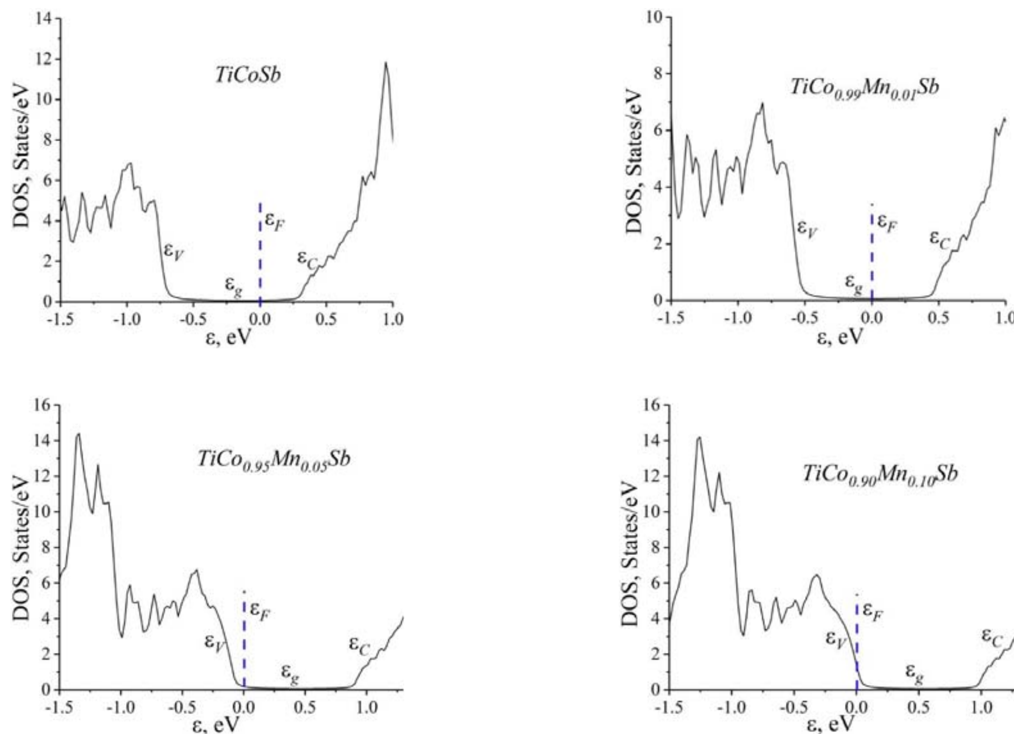

Fig. 3. Distribution of density of electronic states DOS for an ordered variant of the $TiCo_{1-x}Mn_xSb$ structure

Approaching the Fermi level ε_F to the percolation level of the valence band ε_V will lead to the sign inversion of the Seebeck coefficient α(T, x) from negative to positive, and the Fermi level ε_F crossing the percolation level of the valence band ε_V will change the conduction of the $TiCo_{1-x}Mn_xSb$ semiconductor from activation to metal type [4, 13]. That is, in the experiment the activation parts will disappear on the dependences ln(ρ(1/T)), and the values of the resistivity ρ will increase with temperature.

The calculation of distribution of the density of electronic states DOS for the ordered variant of the crystal structure of the thermoelectric material $TiCo_{1-x}Mn_xSb$ allows modeling the behavior of electrokinetic characteristics (Fig. 4). In Fig. 4*a*, as an example, the results of variation of the Seebeck coefficient α(x,T) are shown at different impurity concentrations and temperatures. As expected, the values α(x,T) are positive at all concentrations and temperatures, and the maximum values α(x,T) are reached at concentration $x \approx 0.08$. At the concentrations of *Mn* atoms, $x \approx 0.08–0.10$, the values of the thermoelectric power factor $Z^*_{calc.}$ increase rapidly (Fig. 4b).

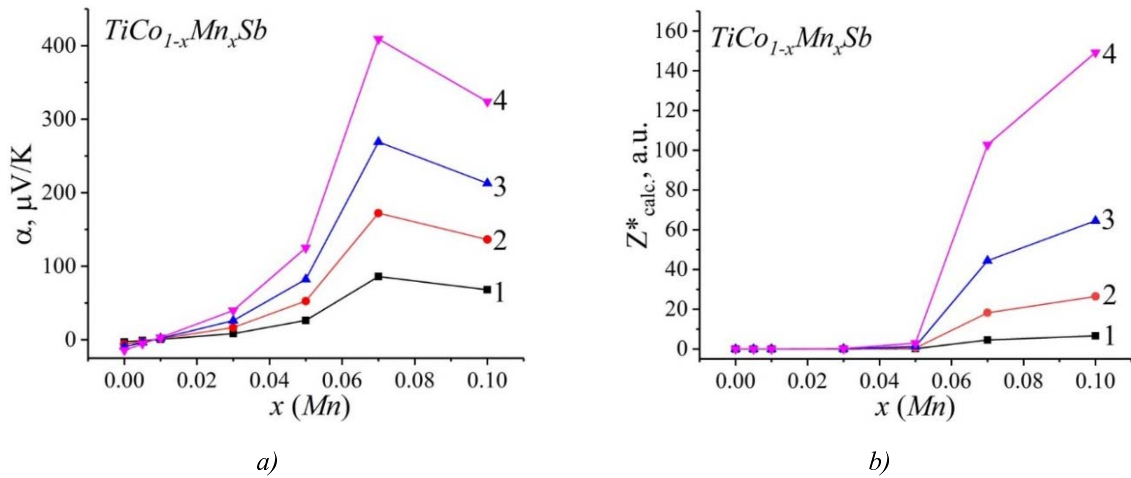

Fig. 4. Modeling of variation of the Seebeck *coefficient α (**a**) and the thermoelectric power factor $Z^*_{calc.}$ (**b**) for an ordered variant of the $TiCo_{1-x}Mn_xSb$ structure at temperatures: 1 – 80 K; 2 – 160 K; 3 – 250 K; 4 – 380 K*

Investigation of the electrokinetic and energy characteristics of *TiCo1-xMnxSb*

Temperature and concentration dependences of electrical resistivity ρ and the Seebeck coefficient α for $TiCo_{1-x}Mn_xSb$ are given in Figs. 5–7.

The temperature dependence of the electrical resistivity ln(ρ(1/T)) for *TiCoSb* (Fig. 5) is typical for doped and compensated semiconductors and is described by known relation [13]:

$$\rho^{-1}(T) = \rho_1^{-1} \exp\left(-\frac{\varepsilon_1^{\rho}}{k_B T}\right) + \rho_3^{-1} \exp\left(-\frac{\varepsilon_3^{\rho}}{k_B T}\right), \tag{1}$$

where the first high-temperature term describes the activation of current carriers ε_1^{ρ} = 100.6 meV from the Fermi level ε_F to the percolation level of the conduction band ε_C, and the second term, at low temperatures, – the hopping conduction with energy ε_3^{ρ} = 5.1 meV at donors impurity states. As seen from Fig. 5, for $TiCo_{1-x}Mn_xSb$ samples, except for the sample at x=0.05, the dependences ln(ρ(1/T)) are also described by relation (1).

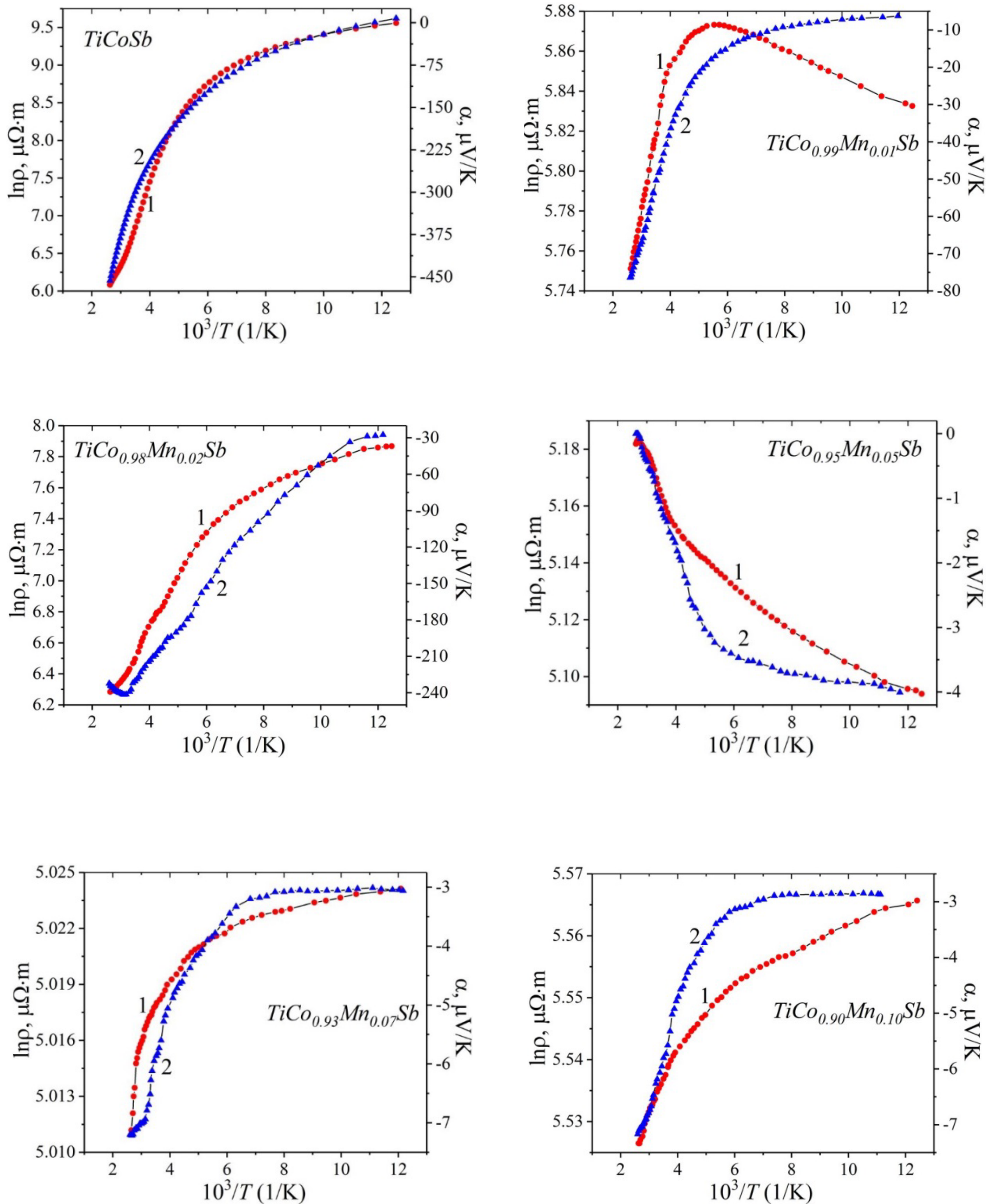

Fig. 5. Temperature dependences of electrical resistivity ln(ρ(1/T)) and the Seebeck coefficient α(1/T) of thermoelectric material $TiCo_{1-x}Mn_xSb$

The variation of the Seebeck coefficient values α(1/*T*) for $TiCo_{1-x}Mn_xSb$ (Fig. 5) is also a classic for doped and compensated semiconductors and is described by the relation [14]:

$$\alpha = \frac{k_B}{e}\left(\frac{\varepsilon_i^{\ \alpha}}{k_B T} - \gamma + 1\right), \qquad (2)$$

where γ is a parameter that depends on the nature of scattering. From the temperature dependence of α(1/*T*) of *TiCoSb* at high temperatures, the value of activation energy ε_1^{α} = 214.1 meV is calculated, which is proportional to the amplitude of large-scale fluctuations of the continuous energies bands of heavily doped and highly compensated semiconductor [4, 13]. In turn, from the low-temperature dependence α(1/*T*) at low temperatures, the value of activation energy ε_3^{α} = 10.2 meV is determined, which is proportional to the amplitude of modulation of small-scale fluctuation of HDHCS [4, 13].

The results of measuring the electrokinetic characteristics for the initial *TiCoSb* semiconductor are fully consistent with those previously obtained in Refs. [3–9]. The high compensation of *TiCoSb* (closeness of concentrations of ionized acceptors and donors) is evidenced by the character of the variation of the Seebeck coefficient α (Figs. 5, 6). Indeed, *TiCoSb* is a semiconductor of the hole-type conduction at temperatures *T* = 80–90 K, as indicated by the positive values of the Seebeck coefficient: $\alpha_{80\ K}$ = 7.75 μV/K and $\alpha_{90\ K}$ = 0.71 μV/K. However, at higher temperatures, the sign of the Seebeck coefficient α of *TiCoSb* becomes negative ($\alpha_{95\ K}$ = -6.33 μV/K), indicating electrons as the majority charge carriers.

Doping the initial semiconductor *TiCoSb* by the lowest concentration of impurity *Mn* atoms, *x* = 0.01, leads to substantial changes in the temperature dependence ln(ρ(1/*T*)) (see Fig. 5). The presence of a high-temperature activation part on the ln(ρ(1/*T*)) dependence for $TiCo_{0,99}Mn_{0,01}Sb$ is evidence of the location of the Fermi level ε_F within the band gap ε_g, and the negative values of the Seebeck coefficient α(*T*,*x*) (Figs. 5, 6) specify its position which is at a distance of ~6 meV from the percolation level of the conduction band ε_C (Fig. 7). In this case, the electrons are the majority carriers of the semiconductor.

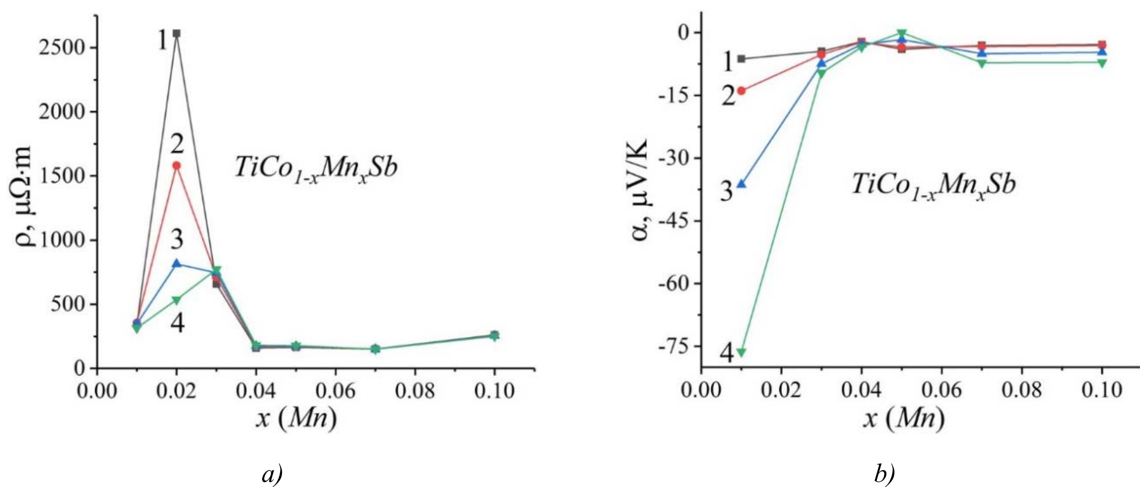

*Fig. 6. Variation of electrical resistivity ρ(x,T) (**a**) and the Seebeck coefficient α(x,T) (**b**) for $TiCo_{1-x}Mn_xSb$ at different temperatures: 1 – 80 K, 2 – 160 K, 3 – 250 K, 4 – 380 K*

The fact that there is no mechanism of hopping conduction ε_3^{ρ} at low temperatures in $TiCo_{0,99}Mn_{0,01}Sb$ (low-temperature activation part is absent on the dependence ln(ρ(1/*T*))) indicates a significant number of donors, which exceeds the concentration of introduced acceptors. There is an overlap of the wave functions of the electrons of impurity states near the Fermi level ε_F, which makes the mechanism of hopping conduction needless [13].

Negative values of the Seebeck coefficient α(*T*,*x*) for $TiCo_{0,99}Mn_{0,01}Sb$ in the temperature range 80–400 K (Figs. 5, 6), when the concentrations of acceptors and donors are close according to DOS calculations (Fig. 3), can be explained by a slightly higher concentration of uncontrolled donors over acceptors. But even at higher impurity *Mn* concentration, in $TiCo_{0,98}Mn_{0,02}Sb$, the sign of the Seebeck coefficient α(*T*,*x*) is negative. An increase in the value of resistivity ρ(*x*,*T*) was observed, for example, at temperature *T* = 80 K from ρ(*x* = 0.01)≈341 μΩ·m to ρ(*x*=0.02) ≈ 2612 μΩ·m (Fig. 6a). This increase in the values of ρ(*x*,*T*) is evidence of an increase in the compensation degree of the semiconductor, which will lead to the appearance of the hopping conduction mechanism ε_3^ρ at low temperatures (low-temperature activation part appears on the dependence ln(ρ(1/*T*))).

The change of the position of the Fermi level ε_F in the sample $TiCo_{0,98}Mn_{0,02}Sb$, which has shifted from the percolation level of the conduction band ε_C at the distance of ~30 meV (Fig. 7), is evidence of an increase of the compensation degree of semiconductor (reduction of the difference between ionized donors and acceptors). Therefore, the increase in the values of the resistivity ρ(*x*,*T*) of $TiCo_{1-x}Mn_xSb$ in the concentration range *x* = 0.01–0.02 is a direct proof of the generation of acceptors in the crystal when the *Co* atoms are substituted by *Mn* atoms. This generation of acceptors leads to the capture of free electrons, which reduces their concentration and causes an increase of the resistivity values ρ(*x*,*T*). On the other hand, the negative values of the Seebeck coefficient α(*x*,*T*) are also experimental evidence that the $TiCo_{1-x}Mn_xSb$ semiconductor has a significant concentration of donors that is greater than the number of introduced acceptors (*x* = 0.02), or in the crystal acceptors and donors are generated simultaneously by different mechanisms.

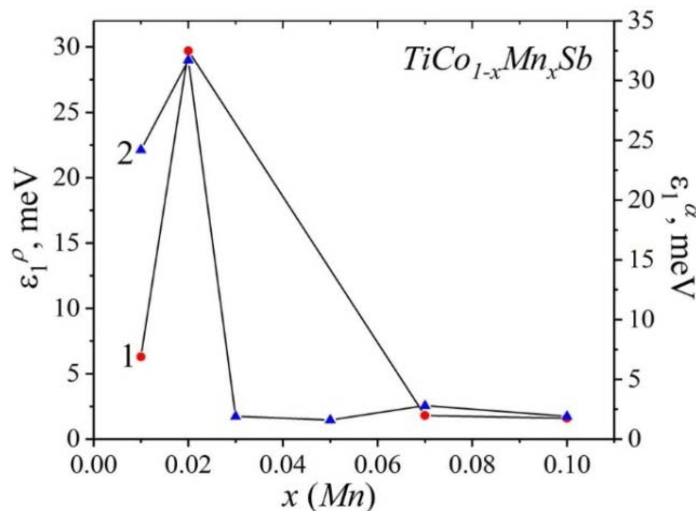

Fig. 7. Variations of the activation energies values ε_1^ρ *(1) and* ε_1^α *(2) for* $TiCo_{1-x}Mn_xSb$

The appearance of the maximum on the dependence of the resistivity ρ(*x*, *T*) of $TiCo_{1-x}Mn_xSb$ (Fig. 6*a*) is an argument that the generation rates of acceptors and donors in the semiconductor are different. At the point of maximum of dependence ρ(*x*, *T*) for $TiCo_{1-x}Mn_xSb$, these rates are balanced. However, the number of acceptors is slightly less than the number of free electrons. This is indicated by the negative values of the Seebeck coefficient α(*x*, *T*) (Fig. 6*b*). Thus, at *T* = 80 K, to balance the ionized acceptors and donors, it is necessary to introduce a concentration of *Mn* atoms (*x* = 0.02) that generates acceptors so that the concentrations of holes and electrons are close. At higher temperatures, ionization of deep donor states takes place, which increases the concentration of electrons, and

therefore it is necessary to introduce a higher concentration of impurity *Mn* atoms into the crystal ($x = 0.03$). It is logical that the maximum on the dependence $\rho(x,T)$ appears at $x = 0.03$ (Fig. 6*a*). The fact of shifting the maximum on the dependence $\rho(x,T)$ with increasing temperature is evidence of the existence of several mechanisms for generating donors of different nature (origin), which generate in the band gap ε_g donor bands ε_D^1 and ε_D^2 of different nature with different depths of their location relative to the percolation level of the conduction band ε_C.

The experimental result described above does not correspond to the conclusions made in the calculations of the electronic structure of the $TiCo_{1-x}Mn_xSb$ semiconductor for the ordered variant of its crystal structure (Fig. 3). When *Co* ($3d^74s^2$) atoms are substituted by *Mn* ($3d^54s^2$) atoms in $TiCo_{1-x}Mn_xSb$, acceptors should be generated in the semiconductor, which will capture all free electrons at concentration $x \approx 0.02$. This process must not be accompanied by inversion of the sign of the Seebeck coefficient α, and free holes will remain the majority charge carriers of the semiconductor (Fig. 4*a*). We can assume that more complex structural changes occur in $TiCo_{1-x}Mn_xSb$ than the substitution of *Co* atoms by *Mn*. At the same time, structural defects of acceptor and donor nature are generated in the crystal by different mechanisms, but the concentration of donors exceeds the concentration of acceptors.

Calculations of the location depth of the Fermi level ε_F relative to the percolation level of the conduction band ε_C of $TiCo_{1-x}Mn_xSb$ at a higher concentration of impurity *Mn* atoms ($x \geq 0.07$) (the sign of the Seebeck coefficient $\alpha(T,x)$ is negative) showed that the Fermi level ε_F very closely approached the percolation level: $\varepsilon_F(x = 0.07) = 1.8$ meV and $\varepsilon_F(x = 0.10) = 1.6$ meV (Fig. 7). The presence of high- and low-temperature activation parts on the $\ln(\rho(1/T))$ dependences of $TiCo_{1-x}Mn_xSb$ at $x \geq 0.07$ is possible provided semiconductor compensation (simultaneous existence of ionized donors and acceptors). However, the fact that the Fermi level ε_F lies within the band gap ε_g near the percolation level of the conduction band indicates a weak compensation of the semiconductor, when the concentration of free electrons is much higher than the concentration of holes.

What is the reason for such, at first glance, illogical behavior of electrokinetic and energy characteristics in the semiconductor thermoelectric material $TiCo_{1-x}Mn_xSb$?

If we remind that in the structure of the base semiconductor *TiCoSb* there are simultaneously ~1% of vacancies in position 4*a* of the *Ti* atoms that generate acceptors, and in the tetrahedral voids of the structure there are ~1% of additional *Co** atoms that generate donors [3], the situation becomes clearer. In turn, structural studies of $TiCo_{1-x}Mn_xSb$ showed that the introduction of impurity *Mn* atoms into the disordered structure of the base semiconductor *TiCoSb* is accompanied by its ordering. This means that the vacancies in position 4*a* of the *Ti* atoms, and also the corresponding acceptor band ε_A disappear. Instead, the *Ti* atoms occupying the vacancies in position 4*a* are a source of electrons that generates the donor band ε_D^1. Partial occupation of tetrahedral voids of the structure by impurity *Mn* atoms is a mechanism of the formation of another donor band ε_D^2.

Conclusions

The result of a complex investigation of the crystal and electronic structures, electrokinetic and energy characteristics of the thermoelectric material $TiCo_{1-x}Mn_xSb$ is the establishment of the nature of structural defects of donor and acceptor nature. It was shown that doping of the base semiconductor *TiCoSb* by *Mn* atoms simultaneously generates the acceptor band ε_A (substitution of *Co* atoms by *Mn*) and the donor bands ε_D^1 and ε_D^2 of different nature. The ratio of the concentrations of ionized acceptors and donors generated in $TiCo_{1-x}Mn_xSb$ determines the position of the Fermi level ε_F and the

mechanisms of electrical conduction. However, this issue requires additional research, in particular, modeling the electronic structure of thermoelectric material under different conditions of introduction into the structure and concentrations of impurity *Mn* atoms. The investigated $TiCo_{1-x}Mn_xSb$ solid solution is a promising thermoelectric material.

References

1. Anatychuk L.I. (1979). *Termoelementy i termoelectricheskiie ustroistva. Spravochnik.* [*Thermoelements and thermoelectric devices*. *Reference book]*. Kyiv: Naukova dumka [in Russian].
2. Romaka V.V., Romaka L.P., Krayovskyy V.Ya., Stadnyk Yu.V. (2015). *Stanidy ridkisnozemelnykh ta perekhidnykh metaliv* [*Stannides of rare earth and transition metals]* Lviv: Lvivska Polytechnika [in Ukrainian].
3. Romaka L.P., Shelyapina M.G., Stadnyk Yu.V., Fruchart D., Hlil E.K., Romaka V.A. (2006). Peculiarity of metal–insulator transition due to composition change in semiconducting $TiCo_{1-x}Ni_xSb$ solid solution. I. Electronic structure calculations, *J. Alloys Compd.*, 414, 46–50.
4. Romaka V.A., Stadnyk Yu.V., Krayovskyy V.Ya., Romaka L.P., Guk O.P., Romaka V.V., Mykyuchuk M.M., Horyn A.M. (2020). *Novitni termochutlyvi materialy ta peretvoriuvachi temperatury* [*New thermosensitive materials and temperature converters*]. Lviv, Lvivska Polytechnika [in Ukrainian].
5. Stadnyk Yu.V., Romaka V.A., Shelyapina M.G., Gorelenko Yu.K., Romaka L.P., Fruchart D., Tkachuk A.V., Chekurin V.F. (2006). Impurity band effect on $TiCo_{1-x}Ni_xSb$ conduction. Donor impurities. *J. Alloys Compd.*, 421, 19–23.
6. Romaka V.A., Stadnyk Yu.V., Fruchart D., Tobola J., Gorelenko Yu.K., Romaka L.P., Chekurin V.F., Horyn A.M. (2007). Features of doping the *p-TiCoSb* intermetallic semiconductor with a *Cu* donor impurity. 1. Calculation of electron structure. *Ukr. J. Phys*., 52(5), 453–457.
7. Romaka V.A., Stadnyk Yu.V., Fruchart D., Tobola J., Gorelenko Yu.K., Romaka L.P., Chekurin V.F., Horyn A.M. (2007). Specific features of doping the *p-TiCoSb* intermetallic semiconductor with a *Cu* donor impurity. 2. Experimental Studies. *Ukr. J. Phys*., 52(7), 650–656.
8. Romaka V.A., Stadnyk Yu.V., Akselrud L.G., Romaka V.V., Frushart D., Rogl P., Davydov V.N., Gorelenko Yu.K. (2008). Mechanism of local amorphization of a heavily doped $Ti_{1-x}V_xCoSb$ intermetallic semiconductor. *Semiconductors*, 42(7), 753–760.
9. Romaka V.A., Stadnyk Yu.V., Romaka L.P., Krayovskyy V.Ya., Romaka V.V., Horyn A.M., Konyk M.B., Romaniv I.M., Rokomaniuk M.V. (2019). Features of structural, energetic and magnetic characteristics of thermoelectric material $Ti_{1-x}Sc_xCoSb$. *J. Thermoelectricity*, 1, 25–41.
10. Roisnel T., Rodriguez-Carvajal J. (2001). WinPLOTR: a windows tool for powder diffraction patterns analysis. *Mater. Sci. Forum*, Proc. EPDIC7 378–381, 118–123.
11. Schruter M., Ebert H., Akai H., Entel P., Hoffmann E., Reddy G.G. (1995). First-principles investigations of atomic disorder effects on magnetic and structural instabilities in transition-metal alloys. *Phys. Rev*. B 52, 188–209.
12. Moruzzi V.L., Janak J.F., Williams A.R. (1978). *Calculated electronic properties of metals.* NY: Pergamon Press.
13. Shklovskii B.I. and Efros A.L. (1984). *Electronic properties of doped semiconductors* NY: Springer; (1979) Moscow: Nauka.
14. Mott N.F., Davis E.A. (1979). *Electron processes in non-crystalline materials.* Oxford: Clarendon Press.

Submitted 30.06.2020

Ромака В.А., *док. тех. наук***,** *професор*[1]
Стадник Ю.В., *канд. хім. наук*[2]
Ромака Л.П., *канд. хім. наук*[2]
Горинь А.М., *канд. хім. наук*[2]
Романів І.М., *канд. хім. наук*[2],
Пашкевич В.З., *канд. техн. наук*[1]
Гопернюк А.Я., *канд. техн. наук*[1]

[1]Національний університет “Львівська політехніка”
вул. С. Бандери, 12, Львів, 79013, Україна,
e-mail: vromaka@polynet.lviv.ua;
[2]Львівський національний університет ім. І. Франка
вул. Кирила і Мефодія, 6, Львів, 79005, Україна;
e-mail: lyubov.romaka@lnu.edu.ua

ДОСЛІДЖЕННЯ ЕНЕРГЕТИЧНИХ ТА КІНЕТИЧНИХ ХАРАКТЕРИСТИК ТЕРМОЕЛЕКТРИЧНОГО МАТЕРІАЛУ $TiCo_{1-x}Mn_xSb$

Досліджено кристалічну та електронну структури, температурні і концентраційні залежності питомого електроопору та коефіцієнта термо-ерс термоелектричного матеріалу $TiCo_{1-x}Mn_xSb$, x = 0.01–0.10, у діапазоні температур T = 80–400 K. Показано, що легування базового напівпровідника TiCoSb атомами Mn супроводжується одночасним генеруванням структурних дефектів акцепторної та донорної природи та появою в забороненій зоні акцепторної ε_A (заміщення атомів Co на Mn) і донорних зон ε_D^1 та ε_D^2 різної природи. Співвідношення генерованих у $TiCo_{1-x}Mn_xSb$ концентрацій іонізованих акцепторів і донорів визначає положення рівня Фермі ε_F та механізми електропровідності термоелектричного матеріалу. Бібл. 14, рис. 7.

Ключові слова: електронна структура, електроопір, коефіцієнт термоЕРС.

Ромака В.А., *док. тех. наук***,** *профессор*[1]
Стаднык Ю.В., *канд. хим. наук*[2]
Ромака Л.П., *канд. хим. наук*[2]
Горынь А.М., *канд. хим. наук*[2]
Романив И.М., *канд. хим. наук*[2],
Пашкевич В.З., *канд. техн. наук*[1]
Гопернюк А.Я., *канд. техн. наук*[1]

[1]Национальный университет "Львовская политехника",
ул. С. Бандеры, 12, Львов, 79013, Украина,
e-mail: vromaka@polynet.lviv.ua;
[2]Львовский национальный университет имени Ивана Франко,
ул. Кирилла и Мефодия, 6, Львов, 79005, Украина,
e-mail: lyubov.romaka@lnu.edu.ua;

ИССЛЕДОВАНИЕ ЭНЕРГЕТИЧЕСКИХ И КИНЕТИЧЕСКИХ ХАРАКТЕРИСТИК ТЕРМОЭЛЕКТРИЧЕСКИХ МАТЕРИАЛОВ $TiCo_{1-x}Mn_xSb$

Исследованы кристаллическая и электронная структуры, температурные и концентрационные зависимости удельного электросопротивления и коэффициента термоЭДС термоэлектрического материала $TiCo_{1-x}Mn_xSb$, x = 0.01 – 0.10, в диапазоне температур T = 80 – 400 K. Показано, что легирования базового полупроводника TiCoSb атомами Mn сопровождается одновременным генерированием структурных дефектов акцепторной и донорной природы и появлением в запрещенной зоне акцепторной ε_A (замещение атомов Co на Mn) и донорных зон ε_D^1, ε_D^2 различной природы. Соотношение генерируемых в $TiCo_{1-x}Mn_xSb$ концентраций ионизированных акцепторов и доноров определяет положение уровня Ферми ε_F и механизмы электропроводности термоэлектрического материала. Библ. 14, рис. 7.

Ключевые слова: Электронная структура, электросопротивление, коэффициент термоЭДС

References

1. Anatychuk L.I. (1979). *Termoelementy i termoelectricheskiie ustroistva. Spravochnik.* [*Thermoelements and thermoelectric devices. Reference book]*. Kyiv: Naukova dumka [in Russian].
2. Romaka V.V., Romaka L.P., Krayovskyy V.Ya., Stadnyk Yu.V. (2015). *Stanidy ridkisnozemelnykh ta perekhidnykh metaliv* [*Stannides of rare earth and transition metals]* Lviv: Lvivska Polytechnika [in Ukrainian].
3. Romaka L.P., Shelyapina M.G., Stadnyk Yu.V., Fruchart D., Hlil E.K., Romaka V.A. (2006). Peculiarity of metal–insulator transition due to composition change in semiconducting $TiCo_{1-x}Ni_xSb$ solid solution. I. Electronic structure calculations, *J. Alloys Compd.*, 414, 46–50.
4. Romaka V.A., Stadnyk Yu.V., Krayovskyy V.Ya., Romaka L.P., Guk O.P., Romaka V.V., Mykyuchuk M.M., Horyn A.M. (2020). *Novitni termochutlyvi materialy ta peretvoriuvachi temperatury* [*New thermosensitive materials and temperature converters*]. Lviv, Lvivska Polytechnika [in Ukrainian].
5. Stadnyk Yu.V., Romaka V.A., Shelyapina M.G., Gorelenko Yu.K., Romaka L.P., Fruchart D., Tkachuk A.V., Chekurin V.F. (2006). Impurity band effect on $TiCo_{1-x}Ni_xSb$ conduction. Donor impurities. *J. Alloys Compd.*, 421, 19–23.
6. Romaka V.A., Stadnyk Yu.V., Fruchart D., Tobola J., Gorelenko Yu.K., Romaka L.P., Chekurin V.F., Horyn A.M. (2007). Features of doping the *p-TiCoSb* intermetallic semiconductor with a *Cu* donor impurity. 1. Calculation of electron structure. *Ukr. J. Phys*., 52(5), 453–457.
7. Romaka V.A., Stadnyk Yu.V., Fruchart D., Tobola J., Gorelenko Yu.K., Romaka L.P., Chekurin V.F., Horyn A.M. (2007). Specific features of doping the *p-TiCoSb* intermetallic semiconductor

with a *Cu* donor impurity. 2. Experimental Studies. *Ukr. J. Phys*., 52(7), 650–656.

8. Romaka V.A., Stadnyk Yu.V., Akselrud L.G., Romaka V.V., Frushart D., Rogl P., Davydov V.N., Gorelenko Yu.K. (2008). Mechanism of local amorphization of a heavily doped $Ti_{1-x}V_xCoSb$ intermetallic semiconductor. *Semiconductors*, 42(7), 753–760.
9. Romaka V.A., Stadnyk Yu.V., Romaka L.P., Krayovskyy V.Ya., Romaka V.V., Horyn A.M., Konyk M.B., Romaniv I.M., Rokomaniuk M.V. (2019). Features of structural, energetic and magnetic characteristics of thermoelectric material $Ti_{1-x}Sc_xCoSb$. *J. Thermoelectricity*, 1, 25–41.
10. Roisnel T., Rodriguez-Carvajal J. (2001). WinPLOTR: a windows tool for powder diffraction patterns analysis. *Mater. Sci. Forum*, Proc. EPDIC7 378–381, 118–123.
11. Schruter M., Ebert H., Akai H., Entel P., Hoffmann E., Reddy G.G. (1995). First-principles investigations of atomic disorder effects on magnetic and structural instabilities in transition-metal alloys. *Phys. Rev*. B 52, 188–209.
12. Moruzzi V.L., Janak J.F., Williams A.R. (1978). *Calculated electronic properties of metals.* NY: Pergamon Press.
13. Shklovskii B.I. and Efros A.L. (1984). *Electronic properties of doped semiconductors* NY: Springer; (1979) Moscow: Nauka.
14. Mott N.F., Davis E.A. (1979). *Electron processes in non-crystalline materials.* Oxford: Clarendon Press.

Submitted 30.06.2020

S.I. Menshikova *cand. phys. - math. sciences*
E.I. Rogacheva *doc. phys. - math. sciences*

S.I. Menshikova

National Technical University "Kharkiv Polytechnic Institute", 2, Kyrpychova Str., Kharkiv, 61002, Ukraine

E.I. Rogacheva

EFFECT OF DEVIATION FROM STOICHIOMETRY ON THERMAL CONDUCTIVITY OF Bi_2Se_3 POLYCRYSTALS

The dependences of electronic and lattice thermal conductivity on the composition (59.9 - 60.0) at. % Se of Bi_2Se_3 polycrystals subjected to a long-term annealing at 650 K. A non-monotonic behavior of these concentration dependences, associated with a change in the phase composition and defect structure under the deviation from stoichiometry, was observed. The boundaries of the Bi_2Se_3 homogeneity region were estimated. The results of the present work confirm those obtained earlier in our study of the effect of deviation from stoichiometry (59.9 - 60.0 at.% Se) on the electrical conductivity, Hall coefficient, Seebeck coefficient and microhardness of Bi_2Se_3 polycrystals after a similar preparation technology. Bibl. 33. Fig. 3.

Keywords: *bismuth selenide, stoichiometry, concentration, defect structure, thermal conductivity*

Introduction

Solid solutions based on the bismuth selenide are the well-known *n*-type thermoelectric (TE) materials for cooling devices [1]. Bi_2Se_3 belongs to a narrow-gap semiconductor group and demonstrates the unique properties of topological insulator (material which is dielectric in the bulk with a metallic layer on the surface) [2]. The efficiency of a TE energy convertor depends on the value of TE figure of merit Z of a TE material ($Z = S^2 \cdot \sigma / \lambda$, where σ and λ are the electrical and thermal conductivities, respectively, S is the Seebeck coefficient).

Bi_2Se_3 is a bertollide [3-5] with the homogeneity region (HR) shifted to the Bi-rich side at $T >$ 675 K [6]. Bi_2Se_3 melts congruently with an open maximum at 979 K [3,7,8], which is deviated from stoichiometry and located at (59.98 ± 0.01) at. % Se [3-6,9].

Bi_2Se_3 always exhibits *n*-type conductivity which is commonly associated with the presence of a large number of Se vacancies (V_{Se1}) [5,6,10-21] acting as donors. The existence of V_{Se1} was confirmed by a number of authors [6,12,15-18,22-24] with the help of different experimental and theoretical methods (scanning tunneling microscopy, measurements of the Hall coefficient in the temperature range 80-330 K, calculation of the formation energies of various types of defects etc.). Later [24-26], the coexistence of V_{Se1} and antisite defects (AD) – bismuth atoms that occupy positions of selenium ones (Bi_{Se}), in the *n*-Bi_2Se_3 was suggested.

The deviation from stoichiometry in chemical compound leads to the appearance of intrinsic defects, the concentration of which varies within the HR of the compound which determines the properties of the TE material. Analysis of the literature showed, that the HR boundaries of the Bi_2Se_3 were determined just for temperatures above 675 K [6], and the boundaries of the maximal HR are (59.984 - 59.997) at.% Se at 900 K. Despite the fact that Bi_2Se_3 is used for TE applications at